The Use of Fluorescent Dyes and Probes in Surgical Oncology

E.A. Te Velde, Th. Veerman, V. Subramaniam, Th. Ruers

Accepted Manuscript

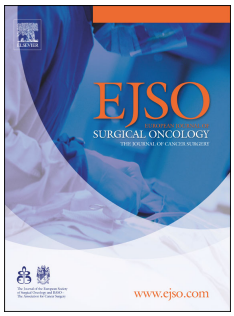

Title: The Use of Fluorescent Dyes and Probes in Surgical Oncology

Authors: E.A. te Velde, Th. Veerman, V. Subramaniam, Th. Ruers

PII: S0748-7983(09)00498-3

DOI: 10.1016/j.ejso.2009.10.014

Reference: YEJSO 2908

To appear in: *European Journal of Surgical Oncology*

Received Date: 23 August 2009

Revised Date: 16October2009

Accepted Date: 22 October 2009

Please cite this article as: te Velde EA, Veerman T, Subramaniam V, Ruers T. The Use of Fluorescent Dyes and Probes in Surgical Oncology, European Journal of Surgical Oncology (2009), doi: 10.1016/j.ejso.2009.10.014

The Use of Fluorescent Dyes and Probes in Surgical Oncology

E. A. te Velde, Th. Veerman, V. Subramaniam,* Th. Ruers

Department of surgical oncology, The Netherlands cancer Institute - Antoni van Leeuwenhoek Hospital, Amsterdam, The Netherlands

**Department of Biophysical Engineering, Faculty of Science and Technology, University of Twente, The Netherlands*

Address of correspondence and requests for reprints:

Dr. T. Ruers

Department of surgical oncology

Antoni van Leeuwenhoek Hospital

PObox 90203

1006 BE Amsterdam

Tel: 0031205122565

Fax: 0031205122554

Abstract

Aims and background: Improved visualization of surgical targets inside of the patient helps to improve radical resection of the tumor while sparing healthy surrounding tissue. In order to achieve an image, optical contrast must be generated by properties intrinsic to the tissue, or require the attachment of special visualization labels to the tumor. In this overview the current status of the clinical use of fluorescent dyes and probes are reviewed.

Methods: In this review, all experimental and clinical studies concerning fluorescent imaging were included. In addition, in the search for the optimal fluorescent imaging modality, all characteristics of a fluorescent dye were described.

Findings and Conclusions: Although the technique of imaging through fluorescence sounds promising and several animal models show efficacy, official approval of these agents for further clinical evaluation, is eagerly awaited.

Introduction

The principles of cancer treatment are radical resection of the primary tumor, with or without its metastases and its draining lymph nodes. In the earlier days, the resections were extensive, but current practice emphasizes sparing healthy tissue as much as possible. Better visualization of surgical targets inside of the patient helps to improve radical resection of the tumor while sparing healthy surrounding tissue. Tumor boundaries are not easily discriminated and their sentinel lymph nodes can be difficult to detect. Improvement of visualization in a non-invasive manner is possible by the use of optical imaging. Optical imaging is defined as a technique that exploits the properties of light emitted from a laser or infrared source to image anatomic or chemical properties of matter. In order to achieve an image, optical contrast must be generated by properties intrinsic to the tissue, or require the attachment of special visualization labels to the tumor. The latter approach, exploiting the luminescence generated by these specific labels, is most commonly used. At this moment there are three major types of labels used in optical imaging: fluorescent proteins, bioluminescence, and fluorescent dyes.[1] Whereas bioluminescence and fluorescent proteins need engineering of cell lines or transgenic animals that carry the appropriate gene, fluorescent dyes do not, and may be unspecifically or specifically targeted to the relevant tissue. This property gives fluorescent dyes the potential for more rapid translation to clinical applications than approaches requiring genetic engineering. In this overview we discuss the current status of the clinical use of these fluorescent dyes.

Methods

A search of Medline and Pubmed databases of studies on fluorescent imaging was performed. All studies were included in this review, in order to give an accurate overview of the current status of the use of fluorescence in tumour models as well as clinical applications. A division was made into imaging of surgical anatomy by Indocyanine Green, dyes and probes that accumulate in the sentinel lymph node, probes that visualize increased cell-metabolism, probes that are activated by tumor-associated proteases and probes that bind to a specific molecular target. In the search for the optimal fluorescent imaging modality, at first, a summary was given to describe the characteristics of a fluorescent dye.

Fluorescent Dye Characteristics

For an optimal image, the fluorescent dye needs to fulfill several criteria with respect to the following characteristics: wavelength, quantum yield, solubility, photobleaching, non-specific binding, signal-to background ratio, clearance and toxicity.

Wavelength: Firstly, fluorescent light needs to propagate a maximum distance through the tissue. Limiting factors for the depth of tissue penetration are absorption and scattering of light;[2] with increasing wavelength (that is in the red or infrared region of the optical spectrum) absorption and scattering of light in tissue decreases. Fluorescent dyes can be designed to emit at a range of different wavelengths spanning the optical spectrum. Below ~700 nm the wavelength of the fluorescent dye is too low to be detected further than a few hundreds of micrometers of tissue penetration.[2] Between 700 nm and 900 nm (the near-infrared region, NIR) absorption is at its lowest. Usage of dyes with wavelengths above 900 nm is not possible because water absorbs very strongly at these wavelengths, dramatically reducing the efficacy of light transmission.[3] In order to maximize the depth of tissue penetration, the most optimal wavelengths for fluorescent dyes used in tissue imaging applications is between 700 and 900nm.[3]

Another requirement of optimal fluorescence imaging is to minimize interference from intrinsic fluorescence (often termed autofluorescence) from the patient's tissue. NIR fluorescent dyes are not hindered by interfering autofluorescence because the patient's tissue generally exhibits negligible emission in this region.[1,4]

Quantum Yield: Another criterion is that the dye should possess a high quantum yield. The fluorescence quantum yield (QY) reflects the efficiency of the fluorescence process. The QY is defined as the ratio of the number of photons emitted to the number of photons absorbed. The maximum fluorescence QY is 1.0 (100%); every photon absorbed results in a photon

emitted. All agents with QY between 0.1 and 1 are considered fluorescent, and all below 0.1 do not have enough emission.

Solubility: It is evident that the dye needs to be soluble for administration into the tissue whether intravascular or into the lymph stream.

Photobleaching: Photobleaching is the photochemical destruction of a fluorophore and may complicate the observation of fluorescent molecules as they will eventually be destroyed by the light exposure (named fluence) necessary to stimulate them into fluorescing. The lower the photo bleaching of the dye, the higher the stability and its potential for practical use.

Non-specific binding: Obviously non-specific binding of the dye should not occur or should only be very minimal.[5] Non-specific binding may occur with cellular membranes, proteins and extra cellular matrix materials. Such non-specific binding results in background fluorescence, which reduces the signal-to-noise ratio and limits tagging specificity and detection sensitivity.

Signal to background ratio: The criteria mentioned above (Wavelength, Quantum Yield, Solubility, Photo bleaching and Non-Specific Binding) all influence the signal-to-background ratio, a quantity that should as high as possible for optimal detection of the fluorescent dye.

Clearance and toxicity: Apart from the physical properties of the dye, practical use of the agent is determined by its toxicity. The clearance of free dyes is one of the parameters for toxicity. Besides, it is also a parameter influencing interfering-background light, as any uncleared free dye will contribute to the background. The optimal dyes should, therefore, have a rapid clearance.

Many NIR fluorescent dyes have been tested for tissue imaging applications thus far, of which the most commonly used dyes are ICG, Cy 5.5, Cy7, Irdye800 CW, and ProSense 750. Recent developments of semiconductor nanocrystals or quantum dots (QDs) have provided an alternative to generate NIR fluorescence contrast. However, none of the dyes have the same

features. These may differ significantly with regard to their fluorescent characteristics, as summarized in table 1.

Wavelength

All the dyes have wavelengths between 700-900 nm, except for Cy5.5, that has a emission wavelength of 695 nm.[1] Therefore, Cy5.5 might be influenced by some auto fluorescence. The separation between excitation and emission wavelengths, also known as the Stokes' shift, for all the above-mentioned dyes is large enough to enable efficient filtering of the emitted fluorescence from the excitation light. QDs have an exceedingly excitation or absorption spectrum, and are efficiently excited by excitation wavelengths lower than their emission wavelength.[6] QD's of the same material, but with different sizes, can emit light of different colors, enabling efficient multiplexed imaging of several different QDs with the same excitation wavelength.

Quantum Yield

Each of the dyes considered here possesses a quantum yield above the minimum value of 0.10. However, there is a considerable range in the quantum yields of the dyes. ICG and Irdye800 CW have the lowest QY (respectively 0.13 and 0.15)[7], followed by Cy5.5 and Cy7 (respectively 0.25 and 0.27). The QDs have the highest QY (0.50-0.60), making them highly fluorescent.[4] The quantum yield of ProSense 750 is difficult to measure since it is a quenched dye and is activated only on cleavage. However, its yield is comparable to the industry standard of Cy7.

Aqueous Solubility

ICG, being a disulfonate, is only moderately soluble, however, it can still successfully be administered intravenously (as reviewed in Frangioni 2003).[4] All other cyanines have a good aqueous solubility.[8] The QDs have different aqueous solubility. The first developed QDs had an outer shell that rendered these QDs insoluble. New QDs have improved as they now have an aqueous-compatible organic layer.

Photo Bleaching

All conventional fluorophores are sensitive to photo bleaching, which limits the emitted light or fluence rate to ~ 50 mW/cm^2.[9] This rate is sufficient to permit efficient optical imaging. In contrast, QDs are resistant to photo bleaching, so that fluence rates can be much higher than 50 mW/cm^2. However, at higher fluence rates tissue damage can occur.

Non-Specific Binding

Non specific binding contributes to the background and not to the signal, decreasing the signal to background ratio. Most cyanines have a low non-specific binding.[4] However, ICG is a cyanine with a high affinity for protein, causing a high non-specific binding to proteins.[4] Many older QDs have charged surface groups and, therefore, have a high non-specific binding.[10] QDs are actively researched and continually developed. Recent research indicates that hydroxyl-coated QDs have a 140-fold reduction in non-specific binding relative to that of carboxylated QDs and a 10-20-fold reduction to that of previous generation QDs.[5] This results in a lower non-specific binding for the new QD`s. ProSense 750, being an activator and not a binder, is not influenced by non-specific binding.

Signal to Background Ratio

The criteria mentioned above form the signal in the signal-to-background ratio. ICG scores the lowest at the previous criteria and has, therefore, the lowest ratio while QDs have the highest ratio. The signal-to-background ratio of ProSense 750 is high because the background is nil, as it is only fluorescent when activated.[11]

Clearance of Free Dyes

ICG and the other free cyanines are rapidly cleared from the blood.[4] Their clearance is accomplished by renal filtration and excretion into the bile. The plasma half life is less than a few minutes. The half life in blood for ProSense 750 is 24h. QDs are large structures of 3-20 nm hydrodynamic diameter (HD). QDs are difficult to clear from the circulation because above 3.5 nm HD renal filtration sharply decreases.[4]

Toxicity

ICG has a remarkably good safety record and is the only FDA approved fluorescent dye.[12] Side effects are very low and generally very mild.[13] The toxicity of Cy5.5 is not completely evaluated. Comparative cytotoxic studies in vitro, however, indicate that the toxicity of Cy5.5 is even less than that of ICG.[14] Unpublished animal studies showed no specific toxicity of the one of the latest cyanines Irdye800 CW. For ProSense 750, phase 1 studies are in progress (data from manufacturer). The toxicological properties have not been investigated thoroughly yet. QDs have characteristics that could render them potentially dangerous.[15] One of them is the low renal clearance. The other is that QDs contain metals that, in their elemental forms, are toxic.[4] Especially the potential toxicity of cadmium or selenium containing QDs remains a major problem for human use.[15]

Targets for Fluorescent Dyes and Probes

Fluorescent dyes can be conjugated to specific substrates to form a probe to visualize specific tumor targets. Fluorescent dyes and probes have different mechanisms of functioning or targeting. Here, we differentiate five categories:

1. Imaging of surgical anatomy by Indocyanine Green
2. Dyes and probes that accumulate in the sentinel lymph node
3. Probes that visualize increased cell-metabolism
4. Probes that are activated by tumor-associated proteases
5. Probes that bind to a specific molecular target

Imaging of Surgical Anatomy by Indocyanine Green

Indocyanine green (ICG) has been used for vascular mapping[16-18], angiograms of the eye[19,20] and angiograms of the brain[21,22]. In oncology, identification of hepatic segments and subsegments for facilitation of hepatic resection was performed in 35 patients with malignant liver disease. [23] The real-time imaging technique proved to be safe and reproducible. ICG was injected into the patient's portal vein branch and images were produced with a special camera. This camera, a Photodynamic Eye (PDE, Hamamatsu Photonics, Hamamatsu, Japan.) consists of a charge-coupled device (CCD) camera surrounded with LEDs that emitted light at a wavelength of 760 nm. The procedure showed accurate liver anatomy in 33 of the 35 patients (94,3%). In one patient a blockage of the portal flow occurred and in another a technical failure of the injection, causing failure of the real-time imaging.

Dyes and Probes That Accumulate in the Sentinel Lymph Node

The SLN is the first lymph node that receives lymphatic drainage from a solid tumor. If in the examination of the SLN no malignant cells are detected, lymphatic metastases can be excluded.[24] In several cancers, such as breast cancer and to a lesser extent melanoma, detection of the SLN has become the clinical standard. For mapping the entire lymphatics, a probe should be small enough so that it can spread through the lymph nodes and image all the small branches. In contrast, to identify and map the Sentinel Lymph Node (SLN) the dye should be large enough to be retained inside the lymph nodes.

The current procedure of SLN mapping is performed with a combination of preoperative nanocolloid injection and intra-operative injection of methylene blue.[25] Although mostly very accurate, unfortunately there are still some disadvantages of the currently-used procedure. The use of the tracer can be logistically complicated when administered a day before the operation by a nuclear medicine physician. It exposes patient and caregivers to a very low amount of ionizing radiation. In addition, the real time imaging with methylene blue is not always very sensitive.[26] It can also result in false-positive nodes because the small dye particles can be readily diffused through the true SLN and traverse multiple nodes.[27] The blue dye does not have optimal tissue contrast.[28] Most important, the blue dye when injected into the dermis colors the skin of the patient for several months.

Fluorescent dyes and probes can be used for mapping of the SLN and some authors claim that it can eliminate the need of radioactive tracers and blue dye.[29] For successful application of fluorescent dyes or probes, three features are important: median hydrodynamic diameter, absence of surface charge, and high contrast generation.[7] In the paragraphs below the different dyes and probes and their modes of functioning are discussed.

Dyes

The feasibility of ICG for lymphatic imaging was already demonstrated in several animal studies. Ogata et al. detected superficial lymphatic vessels in a rat model with a minimal diameter of 0.1 mm.[13] The sensitivity of detecting vessels seems to be almost 100% since they identified ICG fluorescence from lymphatic vessels in all of the examined animals. The ICG remained inside the lymphatic vessels for at least ten minutes. The specificity is presumed to be 100% because when ICG is injected into arteries or veins instead of the lymphatics, the dye is immediately washed away within a minute, causing immediate blurring and disappearance of the fluorescence.

The first use of ICG in human SLN mapping was done by Motomura et al. (1999).[30] The SLN biopsy was guided by ICG in 172 patients with stage I or II breast cancer. The ICG was injected into the breast parenchyma surrounding the primary tumor. However, the SLNs were resected without the use of NIR light due to the lack of a special camera and were identified by eye. Thus, SLNs were only identified in 127 of 172 patients (73,8%) with a false-negative rate of 11.1%, defined as a negative SLN with positive lymph nodes in the axillary dissection specimen.

Dissection of the fluorescent SLN by fluorescence navigation was initiated by Kitai et al. (2005).[31] The images were obtained by a prototype charge-coupled device (CCD) camera surrounded with LEDs that emitted light at a wavelength of 760 nm. Eighteen patients with stage I or II breast cancer were injected subcutaneously around the areola with ICG. Visualization of nodes without the camera was successful in 50% of the patients, whereas the use of the imaging system increased the identification rate to 94%. These authors did not report false-negative SLN's.

In 2008, Tagaya et al. mapped the SLN with ICG and used a blue dye (indigo carmine) as a control.[32] The dyes were injected subdermally at the same time around the areola. The image

was produced by a more sophisticated camera, the Photodynamic Eye (PDE, Hamamatsu Photonics, Hamamatsu, Japan.). The SLNs were detected under fluorescence guidance in all 25 patients, resulting in a detection rate of 100% without false negative nodes and without any need for training. The control group using blue dye only detected lymph nodes in 92% with a false negative percentage of 11.8. Lowering the dose of ICG in this model was found by others to lead to lower efficacy.[33] Interestingly, in a study on lymphatic drainage the network could be observed in 89.2% of all patients, however in the tumor area, only in 12 of 33 patients could lymphatic pathways be observed.[34] Although this observation may deepen the apprehension of lymphatic drainage of the tumour in general, it may not be clinically relevant for detection and resection of the SLN(s).

In a small series of ten skin cancer patients, ICG fluorescence guided by PDE was successfully used to map the SLNs in all ten patients.[35] In this study, the SLNs remained fluorescent for over three hours.

In gastric cancer SLNs were detected by ICG and PDE in 90.9% and colorectal cancer in 88.5% of monitored patients.[36] However, in these patients very high false negative rates were found (70.0 % for gastric cancer and 66.7% for colorectal cancer), since many of the detected lymph nodes were not the true SLN. The accuracy of SLN detection for patients with T1 stage colorectal cancer as well T1 stage gastric cancer was better than for the higher staged tumors. In three T1 gastric cancer patients, SLNs were detected by ICG fluorescence imaging in all cases even though the dye was injected a day before the surgery.[37]

In rectal cancer the detection rate of the SLN appeared to be very low; only in seven out of 25 patients (28%) could the SLN be detected.[38]

Probes

The detection time of ICG used as an individual dye in the above mentioned studies differs from several minutes to a day before surgery.[7,37] To increase the detection time, ICG can be conjugated to Human Serum Albumin (HSA). HSA exhibits a long blood half-life and, therefore shows lymphatic accumulation.[39] When injected in melanomas, the ICG:HSA probe conjugate identifies the SLN's and their associated lymphatic channels in less than a minute.[29] A newer conjugate with HSA, the fluorescent dye HSA800 has been tested in pigs' in hind legs and an esophageal SLN model and provided a twofold higher fluorescent yield than earlier conjugates, demonstrating even the ultra-fine lymphatics.[7,40]

Recently, the first human trial in six women with breast cancer was performed using ICG: HSA. 8 of 9 SLNs identified by Tc- 99m sulfur colloid were also identified by fluorescence. Furthermore, fluorescence identified an SLN, confirmed to have cancer in it, that was not identified by Tc-99m sulfur colloid (figure 1).[41]

By combining two fluorescent dyes with different wavelengths, i.e. Cy5.5 and Cy7, coupled to immunoglobulin G in postmortem athymic mice multicolor visualization of lymphatics has been demonstrated.[42] By labeling different pathways of lymphatics, theoretically disruption of the lymphatics of normal organs can be avoided and thereby reduction of lymphedema can be achieved.

Furthermore, dyes as Cy5.5 have been conjugated to a protected graft copolymer (PGC).[43] PGC is a macromolecule, that when administered intravenously has a long blood half-life and collects in lymph nodes. This could be of help during minimally invasive procedures, since there is no need for peri-tumoral injection.

In theory, the use of QDs for detection of SLNs yields optimal performance. Because of their large diameter the retention in the SLN of QDs is 100%. In addition, their contrast is very high, in multicolor and without fading due to photobleaching.[29,44,45] Furthermore, there is

no need for conjugation. However, as mentioned before, QDs have unknown toxicity and are composed of potentially toxic metals, thus lacking current potential for clinical application.[15] In rats as well as pigs, one research group has studied lymphatic mapping in skin, esophagus, lung, gastro-intestinal tract, pleural pace, peritoneal space, limb, and mammary tissue.[45]

Probes That Image Increased Cell-Metabolism

Optical imaging can also exploit probes that image increased glucose metabolism of the tumor. Tumor cells often have an increased glucose metabolism due to their preferential use of glycolysis for energy generation and to the overexpression of glucose transporters (GLUTs).[46] The most commonly used agent to measure increased glucose metabolism is 2-deoxy-2-[^{18}F]fluoro-D-glucose which is widely used in tumor diagnosis, staging, and monitoring therapeutic response.[47,48] The imaging is done by the use of positron emission tomography (PET).[47] However, PET scanning cannot be used real-time and spatial resolution is relatively low. For optical imaging, two NIR deoxyglucose analogues have been synthesized and will be discussed below.

The first deoxyglucose analogue is Pyro-2DG. The fluorescent moeity that was used for Pyro-2DG is pyropheophorbide and emits in the NIR wavelength range. The probe is accumulated in the tumor through the GLUTs and thereafter retained in the tumor by phosphorylation by hexokinase. Zhang et al. (2004) have found in the glioma bearing rat model as well as in MTB/TOM bitransgenic mice that Pyro-2DG selectively accumulates in the tumor compared to surrounding normal tissue at a ratio of 10:1.[49] Since there is a high discriminative potential, mapping with a high signal-to-noise ratio in that study was possible.

Coupled to Cy5.5 the tumor-targeting ability of the deoxyglucose analogue 2DG was tested in cell cultures as well as in glioblastoma bearing nude mice.[47] The 2DG-Cy5.5 did accumulate in tumor cells, although GLUTs were not the responsible transporter in this

model, and the mechanism of accumulation remained unresolved. The fluorescent Cy5.5 appeared to be too large to be trapped by the GLUTs and therefore it cannot be used as a marker for GLUTs over-expression.

Probes That Are Activated by Tumor-Associated Proteases

Many tumors are known to have increased levels of proteolytic enzymes.[50] These tumor-associated proteases function at multiple stages, affecting tumor establishment, growth, angiogenesis, intravasation, extravasasion, and metastasis.[50]

Probes designed to be solely activated by a specific protease in theory are tumor specific. Only after interaction with the proteases do the probes become fluorescent. Three probes have been designed so far by one research group and they are all activated by protease Cathepsin B.[51-56] This protease is known to be up-regulated in areas of inflammation, necrosis, angiogenesis and focal invasion.[57] Being optically silent when injected, the probes have a low background signal which results in higher signal-to-background ratios when compared to non-specific probes.

For this approach Cy5.5 can be bound to a long circulating and large protected graft copolymer (PGC) in such a way that cleavage of this binding is induced by the tumor protease Cathepsin B.[43] In breast carcinomas and LX-1 small cell carcinomas of nude mice, cleavage of Cy5.5 from the PGC leads to a 12 fold increase in NIR fluorescence signal.[51]

In 2002, Cy5.5-PGC-Cathepsin B imaging was used to discriminate adenomatous polyps in APC-mice from normal mucosa.[53] This study provided opportunities for selective removal of polyps, thereby reducing the transformation of polyps to colorectal cancer.[53]

More recent probes using this concept are the ProSense 680 and 750 dyes (Visen medical). The process of cleavage is identical to Cy5.5-PGC. ProSense consists of graft copolymers coupled to quenched fluorochromes that are released after Cathepsin B cleavage. In mice,

selective tumor imaging can be obtained by ProSense 680 imaging of Cathepsin B expressing lung tumors.[54] The tumoral protease activity was used to improve the detection of small peripheral lung cancer in the Lewis Lung Carcinoma model by use of a novel ProSense 750.[55] In this study, the imaging was performed by NIR microcatheters during thoracoscopy. ProSense 750 was also used in combination with a hand-held imaging device to detect residual sarcoma tissue during surgery in mice.[56] In addition, in combination with fluorescence tomography, it enabled visualization of lung metastasis of the resected sarcomas. Due to its sensitivity, molecular specificity, favorable pharmacokinetics and lack of toxicity, ProSense 750 emerges as a promising clinical imaging agent.[8] Until now, however, these probes have only been tested in animal-studies, while Phase I clinical trials are planned to begin in 2009.

The third and last fluorophore, Chlorin e6 (Ce6), is again quenched to PGC.[58] It accumulates in the tumor and is selectively activated by Cathepsin B. Ce6 is a photodynamic agent and in theory can, apart from imaging, be used for therapeutic purposes as well. When it is illuminated by an appropriate wavelength it transfers its energy to a neighboring molecular oxygen, producing cytotoxic singlet oxygen which causes selective tissue damage, the fundamental principle of photodynamic therapy.[58] In mice bearing fibrosarcomas on the hind limb, protease-mediated photodynamic therapy selectively suppressed tumor growth by >50%. When Ce6 is used on its own, it is not very selective, and may cause damage to normal cells as well.

Probes That Bind to a Specific Molecular Target

Besides proteases, there are many more molecules that are preferentially expressed in malignant cells compared to normal cells. Fluorescent dyes conjugated to specific binders can be used to image these tumor specific targets.

Chlorotoxin (CTX) is a small peptide isolated from scorpion venom that binds specifically to gliomas and related cancers.[59] The receptor for chlorotoxin on glioma cells is matrix-metalloproteinase-2 (MMP-2), which is not expressed in normal brain.[59] In phase I clinical trials for human brain cancer therapy TM-601, the synthetic version of chlorotoxin, was tested and no dose-limiting toxicities were observed.[60] Veiseh et al (2007) coupled CTX to Cy5.5 at doses used for optical imaging in several xenograft mice models without detecting any toxicity.[61] They concluded that CTX:Cy5.5 enters mice medulloblastomas at concentrations suitable for real-time imaging and that CTX:Cy5.5 is also capable of illuminating primary prostate cancer, microscopic foci of cancer cells in lymphatic channels and lymph nodes, intestinal neoplasms and rhabdomyosarcomas in mice. Blocking of MMP-2 resulted in reduction of CTX:Cy5.5 binding in vitro as well as in vivo, showing that MMP-2 facilitates the binding of CTX:Cy5.5.[61]

The effective use of fluorescent antibodies to visualize antigens was demonstrated already in 1995.[62] Ballou et al conjugated several antibodies to cyanines in teratocarcinoma and melanoma mice.[61] A more recent article from Liu et al [63] reports conjugation of transferrin and a mouse anti-human CD74 monoclonal antibody to QDs. These constructs were highly specific to tumor cells in vitro.

Integrins are proteins that function as a receptor and play a role in tumor progression, angiogenesis, and metastasis.[64] Integrin αvβ3 is expressed by newly formed tumor microvessels but not by preexisting vessels or by blood vessels in non-neoplastic tissues.[64] Integrin αvβ3 binds peptides that contain the amino acid sequence Arg-Gly-Asp (RGD). Radio labeled-RGD has been used to measure integrin αvβ3 expression. Wang et. al. (2004) successfully used the integrin αvβ3-targeted peptide c(KRGDf) labeled with Cy5.5 and Irdye800 to detect Kaposi sarcomas and melanomas in nude mice .[65] Instead of cyanines, Cai et al. (2005) used QDs as a NIR label.[66] QDs linked to RGD peptides were tested in a mouse

ear tumor model.[67] The purpose of this research was to study the QD's function, helping to ensure regulatory approval of nanoparticles in humans. The QDs did not extravasate and showed selective binding to single cells of tumor neovasculature. Another fluorochrome that was conjugated to RGD peptides is Cy7.[68] In this study the level of integrin expression was used to evaluate anti-integrin therapy. Cy7 proved to have a deeper tissue penetration then Cy5.5. Cy5.5, however, was retained longer in tumor tissue.

In addition, anti-epidermal growth factor receptor (EGFR) antibodies have been conjugated to QDs. EGFR plays an important role in tumor growth and is associated with a more aggressive disease and shortened survival in cancer patients.[69] Wang et al. (2007) bound anti-EGFR antibodies to QDs using streptavidin-biotin linkages.[70] They demonstrated that these functionalized QDs can identify a specific brain tumor biomarker during surgery. In a short period of time of less than 30 minutes EGFR expressing cells in frozen sections were selectively labeled. In addition, some cells were still visible after seven days. The QDs enabled detection of EGFR expressing cells in brain tumors with details to an extent of cellular resolution. Recently, an anti-EGFR antibody (Cetuximab) conjugated to Oregon Green 488 (OG) was used to visualize colorectal tumors in SCID mice. In this study a heterogeneous binding pattern to EGFR expressing tumors was observed.[71] There was a mismatch of Cetuximab:OG uptake in relation to the extent of EGFR expression that might be explained by the tumor's vascularization and necrosis. Gleysteen et al. conjugated Cetuximab to Cy5.5 and used it in SCID mice in a pulmonary metastatic model as well as a model of regional head and neck metastases.[72] In this study, the fluorescence was successfully confirmed by histopathology in all mice.

Other studies focused on HER-2 receptor binding. The HER-2 receptor is a member of EGFR family and plays a role in tumor growth and prognosis.[73,74] Hilger et al. (2004) labeled a widely used HER-2 antibody (Herceptin) to Cy5.5.[14] This probe was injected intravenously

into three HER-2 expressing tumor bearing mice and whole body intensity of fluorescence was higher compared to three mice with normal HER-2 expressing tumors. Herceptin conjugated to the fluorescent dye Rhodamine Green was successfully used as a probe to detect lung metastases expressing HER-2 in mice one day post injection.[75] This probe visualized HER-2 positive pulmonary metastases and not HER-2 negative metastases. Hassan et al. successfully imaged HER-2 overexpression in four female athymic mice with superficial breast cancer using a conjugate of Alexa Fluor 750 with trastuzamab (Herceptin).[76] They designed a new imaging system which obtained three-dimensional images of fluorescence lifetime distributions in mice. Lee et al. (2008) also used Alexa Fluor in mice.[77] They conjugated it with HER-2-specific Affibodies, which are small proteins with a high affinity for HER-2 using another epitope than trastuzamab. The Alexa fluor:affibodies probe imaged subcutaneous xenografts with HER-2 overexpressing cells in vivo during therapy with Herceptin. These probes appeared to be non toxic for HER-2 overexpressing cells.

Considerations for Future Use

At present many effective fluorescent dyes are available within the NIR spectrum. Conjugation of these dyes to tumor specific targeting molecules can lead to highly selective fluorescent imaging of tumor tissue. Furthermore, fluorescent dyes either on their own or after conjugation to macromolecules can result in selective detection of sentinel nodes. These new developments might give the surgeon the opportunity for real-time fluorescence imaging during surgery. Such approaches, directed to specifically visualize tumor tissue, may be helpful to assist during primary tumor resection and may improve the odds of completely removing all tumor tissue whilst sparing healthy tissue. Moreover, these techniques may specifically target the lymph node areas that have to be removed. Such optical imaging

technologies can be implemented in a wide area of surgical oncology ranging from colorectal and breast cancer to urological and gynecological cancers.

Although the technique of imaging through fluorescence sounds promising, the limitations are still considerable. Why are we not already using fluorescence technology more aggressively? After all, it has been around for a long time. There are few clinical studies as yet and studies in mice have huge translational problems to man. The practical applications in real patients are limited, since until now, indocyanine green is the only dye that has been approved for clinical use and its application is limited to sentinel lymph node detection. It is to be expected that soon other agents, such as ProSense, that more specifically visualize tumor tissue will become clinically available. For clinical implementation of these agents more sophisticated cameras have to be developed for intra-operative and laparoscopic use. The main hurdle to be taken, however, will be official approval of these agents for human use, a development eagerly awaited by the surgical community for further clinical evaluation of optical imaging techniques in clinical practice.

	ICG	Cy5.5	Cy7	Irdye800 CW	ProSense 750	QD (quantum dots)
Excitation wavelength pbs nm	779	675	794	775	750	Broad absorption spectrum
Emission wavelength pbs nm	806	695	775	796	780	808
High Quantum Yield	+/-	+	+	+/-	+	++
Aqueous solubility	+/-	+	+	+	+	+
Low photo-bleaching	+	+	+	+	+	++
Low non-specific binding	-	+	+	+	++	++
High Signal-to-Background Ratio	+/-	+	+	++	++	++
Rapid clearance of free dyes	+	+	+	+	+/-	-
Low toxicity	++	++	++	+	+	-
human studies	+	-	-	-	-	-

Table 1. The following characteristics of fluorescent dyes are compared: wavelength, quantum yield, solubility, photo bleaching, non-specific binding, signal-to background ratio, clearance and toxicity.

- none
+/- some
+ reosonable
++ storng

reference	Procedure	Cancer type	Number of patients	dyes	Identification rate	False-Negative rate
30	SLN mapping	Breast Cancer	172	ICG	127/172 (73,8%)	4/45 (11,1%)
31	SLN mapping	Breast Cancer	18	ICG	17/18 (94%)	0/11 (0%)
32	SLN mapping	Breast Cancer	25	ICG Blue dye	25/25 (100%)	0/17 (0%)
33	SLN mapping	Breast Cancer	9	ICG Blue dye Radio-colloid	8/9 (88,9%)	-
34	SLN mapping	Breast Cancer	7	ICG Blue dye Radio-colloid	33/37 (89.2%) periareolar & 12/33 (36.4%) peritumoral	-
35	SLN mapping	Skin Cancer	10	ICG	10/10 (100%)	unknown
36	SLN mapping	Gastric & Colo-rectal Cancer	22 & 26	ICG Blue dye	20/22 (90,9%) & 23/26 (88,5%)	60,0% & 66,7%
37	SLN mapping	Gastric Cancer	3	ICG	3/3 (100%)	unknown
38	SLN mapping	Rectum Cancer	25	ICG	7/25 (28%)	-
23	Hepatic mapping	Liver Cancer	35	ICG	33/35 (94,3%)	-

Table 2. The following characteristics of all clinical studies are compared: Procedure, Cancer type, Number of patients, dyes, Method, Identification rate, False-Negative rate.

Legend to the figure 1.

NIR Fluorescent Sentinel Lymph Node Mapping in Women with Breast Cancer using the FLARE□ Image-Guided Surgery System: Shown are color video images (left), 800 nm NIR fluorescence images (middle) and a pseudo-colored (lime green) merge of the two (right). Injection (top row) of ICG:HSA into the left breast. Image-guided resection in a different patient (bottom row) demonstrates high-resolution capabilities of the FLARE□ imaging system. Arrows = SLN. Adapted from Troyan et al, with permission.

References

1. Kovar JL, Simpson MA, Schutz-Geschwender A et al. A systematic approach to the development of fluorescent contrast agents for optical imaging of mouse cancer models. Anal Biochem 2007; 367:1-12.

2. Licha K. Contrast agents for optical imaging. Topics in Current Chemistry 2002; 222:1-29.

3. Osterman HL, Schutz-Geschwender A. Seeing Beyond the Visible With IRDye Infrared Dyes. LI-COR Biosciences 2007;1-8.

4. Frangioni JV. In vivo near-infrared fluorescence imaging. Curr Opin Chem Biol 2003; 7:626-634.

5. Kairdolf BA, Mancini MC, Smith AM et al. Minimizing nonspecific Cellular Binding of Quantum Dots with Hydroxyl-Derivatized Surface Coatings. Anal Chem 2008; 80:3029-3034.

6. Lim YT, Kim S, Nakayama A et al. Selection of quantum dot wavelengths for biomedical assays and imaging. Mol Imaging 2003; 2:50-64.

7. Ohnishi S, Lomnes SJ, Laurence RG et al. Organic alternatives to quantum dots for intraoperative near-infrared fluorescent sentinel lymph node mapping. Mol Imaging 2005; 4:172-181.

8. Jaffer FA, Libby P, Weissleder R. Molecular imaging of cardiovascular disease. Circulation 2007; 116:1052-1061.

9. Nakayama A, Bianco AC, Zhang CY et al. Quantitation of brown adipose tissue perfusion in transgenic mice using near-infrared fluorescence imaging. Mol Imaging 2003; 2:37-49.

10. Bentzen EL, Tomlinson ID, Mason J et al. Surface modification to reduce nonspecific binding of quantum dots in live cell assays. Bioconjug Chem 2005; 16:1488-1494.

11. Sevick-Muraca EM, Houston JP, Gurfinkel M. Fluorescence-enhanced, near infrared diagnostic imaging with contrast agents. Curr Opin Chem Biol 2002; 6:642-650.

12. Benya R, Quantana J, Brundage B. Adverse reactions to indocyanine green: a case report and a review of the literature. Cathet Cardiovasc Diagn 1989; 17:231-233.

13. Ogata F, Azuma R, Kikuchi M et al. Novel lymphography using indocyanine green dye for near-infrared fluorescence labeling. Ann Plast Surg 2007; 58:652-655.

14. Hilger I, Leistner Y, Berndt A et al. Near-infrared fluorescence imaging of HER-2 protein over-expression in tumour cells. Eur Radiol 2004; 14:1124-1129.

15. Hardman R. A toxicologic review of quantum dots: toxicity depends on physicochemical and environmental factors. Environ Health Perspect 2006; 114:165-172.

16. Borotto E, Englender J, Pourny JC et al. Detection of the fluorescence of GI vessels in rats using a CCD camera or a near-infrared video endoscope. Gastrointest Endosc 1999; 50:684-688.

17. Detter C, Russ D, Iffland A et al. Near-infrared fluorescence coronary angiography: a new noninvasive technology for intraoperative graft patency control. Heart Surg Forum 2002; 5:364-369.

18. Taggart DP, Choudhary B, Anastasiadis K et al. Preliminary experience with a novel intraoperative fluorescence imaging technique to evaluate the patency of bypass grafts in total arterial revascularization. Ann Thorac Surg 2003; 75:870-873.

19. Herbort CP, LeHoang P, Guex-Crosier Y. Schematic interpretation of indocyanine green angiography in posterior uveitis using a standard angiographic protocol. Ophthalmology 1998; 105:432-440.

20. Chen SJ, Lee AF, Lee FL et al. Indocyanine green angiography of central serous chorioretinopathy. Zhonghua Yi Xue Za Zhi (Taipei) 1999; 62:605-613.

21. Haglund MM, Hochman DW, Spence AM et al. Enhanced optical imaging of rat gliomas and tumor margins. Neurosurgery 1994; 35:930-940.

22. Raabe A, Beck J, Gerlach R et al. Near-infrared indocyanine green video angiography: a new method for intraoperative assessment of vascular flow. Neurosurgery 2003; 52:132-139.

23. Aoki T, Yasuda D, Shimizu Y et al. Image-guided liver mapping using fluorescence navigation system with indocyanine green for anatomical hepatic resection. World J Surg 2008; 32:1763-1767.

24. Morton DL, Wen DR, Wong JH et al. Technical details of intraoperative lymphatic mapping for early stage melanoma. Arch Surg 1992; 127:392-399.

25. cox CE, Pendas S, Cox JM et al. Guidelines for sentinel node biopsy and lymphatic mapping of patients with breast cancer. Ann Surg 1998; 227:651-653.

26. Schirrmeister H, Kotzerke J, Vogl F et al. Prospective evaluation of factors influencing success rates of sentinel node biopsy in 814 breast cancer patients. Cancer Biother Radiopharm 2004; 19:784-790.

27. Alazraki NP, Eshima D, Eshima LA et al. Lymphoscintigraphy, the sentinel node concept, and the intraoperative gamma probe in melanoma, breast cancer, and other potential cancers. Semin Nucl Med 2008; 27:55-67.

28. Soltesz EG, Kim S, Kim SW et al. Sentinel lymph node mapping of the gastrointestinal tract by using invisible light. Ann Surg Oncol 2006; 13:386-396.

29. Tanaka E, Choi HS, Fujii H et al. Image-guided oncologic surgery using invisible light: completed pre-clinical development for sentinel lymph node mapping. Ann Surg Oncol 2006; 13:1671-1681.

30. Motomura K, Inaji H, Komoike Y et al. Sentinel node biopsy guided by indocyanine green dye in breast cancer patients. Jpn J Clin Oncol 1999; 29:604-607.

31. Kitai T, Inomoto T, Miwa M et al. Fluorescence navigation with indocyanine green for detecting sentinel lymph nodes in breast cancer. Breast Cancer 2005; 12:211-215.

32. Tagaya N, Yamazaki R, Nakagawa A et al. Intraoperative identification of sentinel lymph nodes by near-infrared fluorescence imaging in patients with breast cancer. Am J Surg 2008; 195:850-853.

33. Sevick-Muraca EM, Sharma R, Rasmussen JC et al. Imaging of lymph flow in breast cancer patients after microdose administration of a near-infrared fluorophore: feasibility study. Radiology 2008; 246:734-741.

34. Ogasawara Y, Ikeda H, Takahashi M et al. Evaluation of breast lymphatic pathways with indocyanine green fluorescence imaging in patients with breast cancer. World J Surg 2008; 32:1924-1929.

35. Fujiwara M, Mizukami T, Suzuki A et al. Sentinel lymph node detection in skin cancer patients using real-time fluorescence navigation with indocyanine green: preliminary experience. J Plast Reconstr Aesthet Surg 2008.

36. Kusano M, Tajima Y, Yamazaki K et al. Sentinel node mapping guided by indocyanine green fluorescence imaging: a new method for sentinel node navigation surgery in gastrointestinal cancer. Dig Surg 2008; 25:103-108.

37. Miyashiro I, Miyoshi N, Hiratsuka M et al. Detection of sentinel node in gastric cancer surgery by indocyanine green fluorescence imaging: comparison with infrared imaging. Ann Surg Oncol 2008; 15:1640-1643.

38. Noura S, Ohue M, Seki Y et al. Evaluation of the lateral sentinel node by indocyanine green for rectal cancer based on micrometastasis determined by reverse transcriptase-polymerase chain reaction. Oncol Rep 2008; 20:745-750.

39. Swart PJ, Beljaars L, Kuipers ME et al. Homing of negatively charged albumins to the lymphatic system: general implications for drug targeting to peripheral tissues and viral reservoirs. Biochem Pharmacol 1999; 58:1425-1435.

40. Parungo CP, Ohnishi S, Kim SW et al. Intraoperative identification of esophageal sentinel lymph nodes with near-infrared fluorescence imaging. J Thorac Cardiovasc Surg 2005; 129:844-850.

41. Troyan SL, Kianzad V, Gibbs-Strauss SL, Gioux S, Matsui A, Oketokoun R, Ngo L,

Khamene A, Azar F, Frangioni JV. The FLARE intraoperative near-infrared fluorescence imaging system: a first-in-human clinical trial in breast cancer sentinel lymph node mapping. Ann Surg Oncol. 2009 Oct;16(10):2943-52.

42. Hama Y, Koyama Y, Urano Y et al. Two-color lymphatic mapping using Ig-conjugated near infrared optical probes. J Invest Dermatol 2007; 127:2351-2356.

43. Josephson L, Mahmood U, Wunderbaldinger P et al. Pan and sentinel lymph node visualization using a near-infrared fluorescent probe. Mol Imaging 2003; 2:18-23.

44. Kim S, Lim YT, Soltesz EG et al. Near-infrared fluorescent type II quantum dots for sentinel lymph node mapping. Nat Biotechnol 2004; 22:93-97.

45. Frangioni JV, Kim SW, Ohnishi S et al. Sentinel lymph node mapping with type-II quantum dots. Methods Mol Biol 2007; 374:147-159.

46. Semenza GL, Artemov D, Bedi A et al. 'The metabolism of tumours': 70 years later. Novartis Found Symp 2001; 240:251-260.

47. Cheng Z, Levi J, Xiong Z et al. Near-infrared fluorescent deoxyglucose analogue for tumor optical imaging in cell culture and living mice. Bioconjug Chem 2006; 17:662-669.

48. Gambhir SS. Molecular imaging of cancer with positron emission tomography. Nat Rev Cancer 2002; 2:683-693.

49. Zhang Z, Li H, Liu Q et al. Metabolic imaging of tumors using intrinsic and extrinsic fluorescent markers. Biosens Bioelectron 2004; 20:643-650.

50. Koblinski JE, Ahram M, Sloane BF. Unraveling the role of proteases in cancer. Clin Chim Acta 2000; 291:113-135.

51. Weissleder R, Tung CH, Mahmood U et al. In vivo imaging of tumors with protease-activated near-infrared fluorescent probes. Nat Biotechnol 1999; 17:375-378.

52. Tung CH, Mahmood U, Bredow S et al. In vivo imaging of proteolytic enzyme activity using a novel molecular reporter. Cancer Res 2000; 60:4953-4958.

53. Marten K, Bremer C, Khazaie K et al. Detection of dysplastic intestinal adenomas using enzyme-sensing molecular beacons in mice. Gastroenterology 2002; 122:406-414.

54. Grimm J, Kirsch DG, Windsor SD et al. Use of gene expression profiling to direct in vivo molecular imaging of lung cancer. Proc Natl Acad Sci U S A 2005; 102:14404-14409.

55. Figueiredo JL, Alencar H, Weissleder R et al. Near infrared thoracoscopy of tumoral protease activity for improved detection of peripheral lung cancer. Int J Cancer 2006; 118:2672-2677.

56. Kirsch DG, Dinulescu DM, Miller JB et al. A spatially and temporally restricted mouse model of soft tissue sarcoma. Nat Med 2007; 13:992-997.

57. Emmert-Buck MR, Roth MJ, Zhuang Z et al. Increased gelatinase A (MMP-2) and cathepsin B activity in invasive tumor regions of human colon cancer samples. Am J Pathol 1994; 145:1285-1290.

58. Choi Y, Weissleder R, Tung CH. Selective antitumor effect of novel protease-mediated photodynamic agent. Cancer Res 2006; 66:7225-7229.

59. Deshane J, Garner CC, Sontheimer H. Chlorotoxin inhibits glioma cell invasion via matrix metalloproteinase-2. J Biol Chem 2003; 278:4135-4144.

60. Mamelak AN, Rosenfeld S, Bucholz R et al. Phase I single-dose study of intracavitary-administered iodine-131-TM-601 in adults with recurrent high-grade glioma. J Clin Oncol 2006; 24:3644-3650.

61. Veiseh M, Gabikian P, Bahrami SB et al. Tumor paint: a chlorotoxin:Cy5.5 bioconjugate for intraoperative visualization of cancer foci. Cancer Res 2007; 67:6882-6888.

62. Ballou B, Fisher GW, Waggoner AS et al. Tumor labeling in vivo using cyanine-conjugated monoclonal antibodies. Cancer Immunol Immunother 1995; 41:257-263.

63. Liu TC, Wang JH, Wang HQ et al. Bioconjugate recognition molecules to quantum dots as tumor probes. J Biomed Mater Res A 2007; 83:1209-1216.

64. Brooks PC, Clark RA, Cheresh DA. Requirement of vascular integrin alpha v beta 3 for angiogenesis. Science 1994; 264:569-571.

65. Wang W, Ke S, Wu Q et al. Near-infrared optical imaging of integrin alphavbeta3 in human tumor xenografts. Mol Imaging 2004; 3:343-351.

66. Cai W, Shin DW, Chen K et al. Peptide-labeled near-infrared quantum dots for imaging tumor vasculature in living subjects. Nano Lett 2006; 6:669-676.

67. Smith BR, Cheng Z, De A et al. Real-time intravital imaging of RGD-quantum dot binding to luminal endothelium in mouse tumor neovasculature. Nano Lett 2008; 8:2599-2606.

68. Wu Y, Cai W, Chen X. Near-infrared fluorescence imaging of tumor integrin alpha v beta 3 expression with Cy7-labeled RGD multimers. Mol Imaging Biol 2006; 8:226-236.

69. Zhang H, Berezov A, Wang Q et al. ErbB receptors: from oncogenes to targeted cancer therapies. J Clin Invest 2007; 117:2051-2058.

70. Wang J, Yong WH, Sun Y et al. Receptor-targeted quantum dots: fluorescent probes for brain tumor diagnosis. J Biomed Opt 2007; 12:044021.

71. Aerts HJ, Dubois L, Hackeng TM et al. Development and evaluation of a cetuximab-based imaging probe to target EGFR and EGFRvIII. Radiother Oncol 2007; 83:326-332.

72. Gleysteen JP, Newman JR, Chhieng D et al. Fluorescent labeled anti-EGFR antibody for identification of regional and distant metastasis in a preclinical xenograft model. Head Neck 2008; 30:782-789.

73. Seshadri R, Firgaira FA, Horsfall DJ et al. Clinical significance of HER-2/neu oncogene amplification in primary breast cancer. The South Australian Breast Cancer Study Group. J Clin Oncol 1993; 11:1936-1942.

74. Ravdin PM, Chamness GC. The c-erbB-2 proto-oncogene as a prognostic and predictive marker in breast cancer: a paradigm for the development of other macromolecular markers--a review. Gene 1995; 159:19-27.

75. Koyama Y, Hama Y, Urano Y et al. Spectral fluorescence molecular imaging of lung metastases targeting HER2/neu. Clin Cancer Res 2007; 13:2936-2945.

76. Hassan M, Riley J, Chernomordik V et al. Fluorescence lifetime imaging system for in vivo studies. Mol Imaging 2007; 6:229-236.

77. Lee SB, Hassan M, Fisher R et al. Affibody molecules for in vivo characterization of HER2-positive tumors by near-infrared imaging. Clin Cancer Res 2008; 14:3840-3849.

	ICG	Cy5.5	Cy7	Irdye800 CW	ProSense 750	QD (quantum dots)
Excitation wavelength pbs nm	779	675	794	775	750	Broad absorption spectrum
Emission wavelength pbs nm	806	695	775	796	780	808
High Quantum Yield	+/-	+	+	+/-	+	++
Aqueous solubility	+/-	+	+	+	+	+
Low photo-bleaching	+	+	+	+	+	++
Low non-specific binding	-	+	+	+	++	++
High Signal-to-Background Ratio	+/-	+	+	++	++	++
Rapid clearance of free dyes	+	+	+	+	+/-	-
Low toxicity	++	++	++	+	+	-
human studies	+	-	-	-	-	-

Table 1. The following characteristics of fluorescent dyes are compared: wavelength, quantum yield, solubility, photo bleaching, non-specific binding, signal-to background ratio, clearance and toxicity.

- none
+/- some
+ reosonable
++ storng

	Procedure	Cancer type	Number of patients	dyes	Method	Identification rate	False-Negative rate
Motomura et al. (1999)	SLN mapping	Breast Cancer	172	ICG	5 ml of ICG injected around the tumor. The SLN located without the use of a camera.	127/172 (73,8%)	4/45 (11,1%)
Kitai et al. (2005)	SLN mapping	Breast Cancer	18	ICG	5 ml ICG injected in the subareolar breast tissue. SLNs were dissected using a prototype PDE camera.	17/18 (94%)	0/11 (0%)
Tagaya et al. (2005)	SLN mapping	Breast Cancer	25	ICG Blue dye	1 ml ICG and 3 ml blue dye injected subdermally around the areola. SLNs were dissected using a PDE camera.	25/25 (100%)	0/17 (0%)
Sevick-Muraca et al. (2008)	SLN mapping	Breast Cancer	9	ICG Blue dye Radio-colloid	Microdose solutions of ICG injected intradermal and intraparenchymal. SLNs were dissected through guidance with a gamma probe and blue dye. After resection SN were imaged for fluorescence with a CCD-camera.	8/9 (88,9%)	-
Ogasawara et al. (2008)	SLN mapping	Breast Cancer	7	ICG Blue dye Radio-colloid	5 ml ICG and blue dye injected around the areola and tumor with a PDE. The SLNs were dissected using a gamma detection probe and the blue dye.	33/37 (89.2%) periareolar & 12/33 (36.4%) peritumoral	-
Fujiwara et al. (2008)	SLN mapping	Skin Cancer	10	ICG	0.6-0.8 ml ICG and blue dye injected intradermally around tumor. SLNs imaged by a PDE camera and the blue dye.	10/10 (100%)	unknown
Kusano et al. (2008)	SLN mapping	Gastric & Colo-rectal Cancer	22 & 26	ICG Blue dye	2 ml ICG injected into the subserosa around the tumor SLNs imaged with PDE camera	20/22 (90,9%) & 23/26 (88,5%)	60,0% & 66,7%
Miyashiro et al. (2008)	SLN mapping	Gastric Cancer	3	ICG	2-4 ml ICG was injected around the tumor. SLNs dissected using a PDE camera	3/3 (100%)	unknown
Noura et al. (2008)	SLN mapping	Rectum Cancer	25	ICG	5 ml of ICG injected into the submucosal layer around the tumor. SLNs were imaged on macroscopy without the use of a camera	7/25 (28%)	-
Aoki et al. (2008)	Hepatic mapping	Liver Cancer	35	ICG	1 ml of ICG injected into the portal vein Imaging by means of a PDE-2 camera.	33/35 (94,3%)	-

Table 2. The following characteristics of all clinical studies are compared: Procedure, Cancer type, Number of patients, dyes, Method, Identification rate, False-Negative rate.

	Color Video	NIR Fluorescence	Color-NIR Merge
Real-Time SLN Identification	QuickTime™ and a TIFF (Uncompressed) decompressor are needed to see this picture.	QuickTime™ and a TIFF (Uncompressed) decompressor are needed to see this picture.	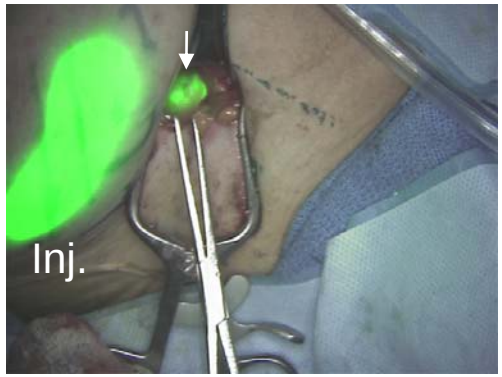
Image-Guided Resection